Comprehensive Molecular and Pathologic Evaluation of Transitional Mesothelioma Assisted by Deep Learning Approach: A Multi-Institutional Study of the International Mesothelioma Panel from the MESOPATH Reference Center

Francoise Galateau Salle, Nolwenn Le Stang, Franck Tirode, Pierre Courtiol, Andrew Nicholson, Ming-Sound Tsao, Henry Tazelaar, Andrew Churg, Sanja Dacic, Victor Roggli, et al.

HHS Public Access

Author manuscript

J Thorac Oncol. Author manuscript; available in PMC 2022 February 23.

Published in final edited form as:

J Thorac Oncol. 2020 June ; 15(6): 1037–1053. doi:10.1016/j.jtho.2020.01.025.

Comprehensive Molecular and Pathologic Evaluation of Transitional Mesothelioma Assisted by Deep Learning Approach: A Multi-Institutional Study of the International Mesothelioma Panel from the MESOPATH Reference Center

A full list of authors and affiliations appears at the end of the article.

Abstract

Introduction: Histologic subtypes of malignant pleural mesothelioma are a major prognostic indicator and decision denominator for all therapeutic strategies. In an ambiguous case, a rare transitional mesothelioma (TM) pattern may be diagnosed by pathologists either as epithelioid mesothelioma (EM), biphasic mesothelioma (BM), or sarcomatoid mesothelioma (SM). This study aimed to better characterize the TM subtype from a histological, immunohistochemical, and molecular standpoint. Deep learning of pathologic slides was applied to this cohort.

Methods: A random selection of 49 representative digitalized sections from surgical biopsies of TM was reviewed by 16 panelists. We evaluated BAP1 expression and *CDKN2A* (p16) homozygous deletion. We conducted a comprehensive, integrated, transcriptomic analysis. An unsupervised deep learning algorithm was trained to classify tumors.

Results: The 16 panelists recorded 784 diagnoses on the 49 cases. Even though a Kappa value of 0.42 is moderate, the presence of a TM component was diagnosed in 51%. In 49% of the histological evaluation, the reviewers classified the lesion as EM in 53%, SM in 33%, or BM in 14%. Median survival was 6.7 months. Loss of BAP1 observed in 44% was less frequent in TM than in EM and BM. p16 homozygous deletion was higher in TM (73%), followed by BM (63%) and SM (46%). RNA sequencing unsupervised clustering analysis revealed that TM grouped together and were closer to SM than to EM. Deep learning analysis achieved 94% accuracy for TM identification.

Conclusion: These results revealed that the TM pattern should be classified as non-EM or at minimum as a subgroup of the SM type.

Keywords

Mesothelioma; Histology; Surgery; Systemic treatment

*Address for correspondence: Francoise Galateau Salle, MD, MESOPATH, MESOBANK, Department of Biopathology, Cancer Center Leon Berard, 28 Rue de Laennec, Lyon 69008, France. francoise.galateau@lyon.unicancer.fr.

Where authors are identified as personnel of the International Agency for Research on Cancer WHO, the authors alone are responsible for the views expressed in this article and they do not necessarily represent the decisions, policy or views of the International Agency for Research on Cancer WHO.

Supplementary Data

Note: To access the supplementary material accompanying this article, visit the online version of the *Journal of Thoracic Oncology* at www.jto.org and at https://doi.org/10.1016/j.jtho.2020.01.025.

Introduction

Even in 2019, malignant pleural mesothelioma (MPM) remains a rare incurable cancer with 30,000 patients diagnosed worldwide, and an expected 26,000 deaths from the disease per year.[1] The incidence is expected to rise until 2030. Histologic subtype epithelioid versus nonepithelioid is a major prognostic factor and decision denominator for all therapeutic strategies. Operation may have a beneficial impact on survival in epithelioid compared with nonepithelioid types; although in nonepithelioid types, systemic therapy (chemotherapy and immunotherapy) strategies are more applicable and frequently used with variable outcomes.[2–8] Recently, the International Mesothelioma Panel (IMP) and the French mesothelioma panel supported by the French National Cancer Institute, the European Reference Network of Rare Cancer, in collaboration with the International Association for the Study of Lung Cancer, conducted a study to evaluate the interobserver agreement in the diagnosis of a random group of 42 surgical biopsy samples diagnosed as biphasic mesotheliomas (BM), that is, combining epithelioid and sarcomatoid morphologic features. The results of the analysis revealed that the identification and recognition of the rare transitional mesothelioma (TM) pattern was challenging for pathologists, diagnosing them either as epithelioid mesotheliomas (EMs), BMs, or sarcomatoid mesotheliomas (SMs). The criteria for the diagnosis of a TM pattern based on expert consensus[9] is mesothelioma that grows in sheets of elongated plump cells (with abundant cytoplasm) that were starting to lose their epithelioid cellular structure but not overtly spindle-shaped and lacking frank sarcomatous features. This pattern was found to be associated with a worse prognosis; the survival for which is very close to that of the SM and pleomorphic types with 0% at 5 years.[9] Taking into account these results, the IMP conducted this new study to further characterize this rare transitional variant.

This study aimed to better define the TM subtype from the structural standpoint and at the transcriptome level. Specific components of the project were (1) to evaluate the interobserver agreement in the diagnosis of TM; (2) to determine which features are used by a group of expert pathologists to make the diagnosis of TM; and (3) to correlate the percentage of TM component with survival. The value of reticulin staining in the separation of TM from EM and SM,[10–12] BAP1 staining, and *CDKN2A*(p16) fluorescence in situ hybridization (FISH) were also assessed.[13–17]

In addition, several articles have highlighted emerging approaches to the diagnosis of MPM, over the past few years, such as RNA sequencing (RNASeq)[18] and artificial intelligence (deep learning).[19] In a groundbreaking article in 2012, Hinton et al.[20] reported that deep learning methods could provide a highly accurate nosologic classification with a very low level of error.[20] Therefore, the final aims of the study were to understand the contribution of RNASeq in the diagnosis and classification of the TM variant, and whether artificial intelligence was capable of identifying this variant and its significance.

Materials and Methods

The study was conducted by the IMP supported by the French National Cancer Institute, The French National health Institute (Santé Publique France), the European Reference

Network of rare cancers, and the International Association for the Study of Lung Cancer. All cases had been classified as mesothelioma after a standardized procedure of certification, collected over 20 years by the National Reference center MESOPATH according to the 2015 WHO Classification.[11,12] Authorization to use human biological samples was obtained (n° AC 2011). Certification was also obtained. The national and local ethics committee (n° DC2008_586, AC-2013-1806, DR-2011-309) of Cancer Center Leon Berard. The representative sections for the interobserver evaluation were scanned using LEICA AT2-400 at 40× magnification, creating whole-slide images (WSI) of the hematoxylin and eosin–stained (H&E) slide.

Case Selection

A random selection of 49 surgical biopsies was identified from the MESOPATH files as having been diagnosed as BM with a TM component by 16 experts of the French Panel of MESOPATH and the IMP on the basis of the WHO 2015 criteria and appropriate phenotype.[11,12,21–33] The criteria for identification of the TM features were selected according to the previous definition of transitional characteristics published in 2018 by Galateau Salle et al.,[9] and were considered as a TM group.[9]

A selection of 49 cases was statistically compared with a total series of 7621 pleural mesotheliomas including 6154 EM, 878 BM, and 540 SM types collected over a study period from January 1998 to June 2016. The 49 cases were required to be surgical biopsy samples and to have H&E sections, formalin-fixed paraffin-embedded (FFPE) blocks and sufficient tumor quantity for additional ancillary techniques. The demographic, clinical, histopathologic, treatment and follow-up characteristics were recorded from the national clinicobiological database of the National French Clinico-Biological Database (MESOBANK). Occupational histories were evaluated by a group of epidemiologists and were available in 71% of the cases. Most cases had conventional and computed tomography images available.

Interobserver Agreement and Delineation of Characteristics

A total of 16 pathologists from the French mesothelioma panel MESOPATH and the IMP with expertise in mesothelioma reviewed the digitally scanned slides (H&E only) without knowledge of previous diagnosis or outcome. A score sheet with 15 items collegially discussed with the IMP was provided to the reviewers (Table 1). Reviewers were first asked to make the following assessments: (1) confirm a diagnosis of MPM; (2) provide the histologic type according to the WHO 2015 classification (EM, BM, or SM); and (3) state whether a TM component was present. The TM pattern could be either diffuse (observed on the totality of the samples), focal (by area of one or several foci of more than 5% of cells), or less than 5% in an individual case (Fig. 1). The second series of questions covered the criteria for cell features defining TM cellular structure (Table 1) and grading of tumor according to Rosen grading.[34] The last question was related to features of “aggressiveness;” that is, the presence or absence of a frank sarcomatous component. Interobserver agreement was evaluated for the final diagnosis of mesothelioma type and on the identification of TM (focal or diffuse).

Reticulin staining was evaluated by Dr. Galateau Salle on a selected series of 10 of 6566 EM cases, 10 of 971 BM, and 10 of 604 SM from the MESOBANK database compared with 10 cases with TM cellular structure. Demographic, clinical, histopathologic, treatment and follow-up data were retrieved from the MESOBANK database.

Immunohistochemical and Molecular Analysis

Staining was performed on 4 μm-thick tissue sections cut from the FFPE block in the Biopathology department of the Cancer Center Leon Berard on the autostainer BenchMark Ventana. The cases exhibited a classical mesothelial immunophenotype; that is, reactivity of both EM and SM components by a broad spectrum of pan-cytokeratin (AE1/AE3), or CK8/18, other PAN-CK (large broad spectrum of cytokeratins) and reactivity for CK5/6 (when available), calretinin nuclear reactivity (with a cutoff of more than 10% reactivity) and Wilm's tumor gene 1 nuclear staining mandatory in the epithelioid component. All the carcinoma markers including CEA, BerEP4, TTF-1, ERα, PAX8, and GATA3 were performed in variable combinations as clinically appropriate[23–30] and failed to react with the tumor cells.

We compared the expression of BAP1 staining, p16 protein expression, and the presence of *CDKN2A* (*p16*) homozygous deletion in the series of 49 TM compared with the data collected from the MESOBANK cohort including 6154 EM, 878 BM, and 540 SM. BAP1 (clone C4) (Santa Cruz: dilution one to 50) nuclear staining was considered positive (when nuclear expression was retained) or negative (complete loss of staining of all tumor cells with a positive internal control on the slides [fibroblast, lymphocytes, etc.]). BAP1 loss could be present in either both components or in the EM component alone.[31–33] p16 protein (clone E6H4) prediluted Ventana was considered positive (diffuse or focal heterogeneous nuclear staining) or negative (for cases showing absence of expression on the tumor cells with a positive internal control on the slides). p16 loss of expression was not considered as a definitive argument of malignancy in the absence of homozygous *CDKN2A* (*p16*) deletion by FISH analysis.[31–33]

CDKN2A (*p16*) FISH for detection of homozygous deletion of *CDKN2A* (*p16*) was performed using the dual-color FISH analysis for the *CDKN2A* locus (9p21) and the centromere of the chromosome 9, using the ZytoVision probe (ZytoLight SPEC *CDKN2A*/CEN 9 Dual Color Probe, # Z-2063-200) on fresh serial recuts of 3 μm to 5 μm in thickness from the FFPE block stored in optimal conditions, as previously described.[9] A minimum of 100 cells and more than 80% of nuclei had to be hybridized. A cutoff value of 20% of nuclei with no *CDKN2A* copy was considered as positive for homozygous deletion in both EM and SM components.

RNASeq expression of 10 cases of mesothelioma of each subtype (EM, SM, and TM) was performed on FFPE material. Libraries were prepared with 100 ng of total RNA using TruSeq RNA Access Library Prep Kit (Illumina, San Diego, CA). Libraries were pooled by groups of 12 samples. Paired end-sequencing was performed using the NextSeq 500/550 High Output V2 kit (150 cycles) on Illumina NextSeq 500 platform (Illumina).[35]

Sequencing data (average of 90 million reads per sample) were aligned with the STAR on GRCh38 reference genome. Expression values were extracted through Kallisto.[36] Clustering analyses were performed by means of Ward agglomerative procedure using 1-Rho (Pearson's correlation value) distances. Consensus clustering was performed using the ConsensusClusterPlus v3.8 R package. Gene ontology analyses were performed online using The Database for Annotation, Visualization and Integrated Discovery v6.7 tool (https://david.ncifcrf.gov/).

AI: Deep Learning Assessment

We assessed whether a machine learning algorithm could be trained to classify tumors with a transitional pattern with high robustness. The algorithm CHOWDER[36] was trained to classify malignant mesothelioma (MM) cases as either TM (n = 35) or non-TM (n = 32) on H&E WSI.

CHOWDER is a novel method specifically designed to address this scenario of nonannotated pathology slides, and train deep learning systems from whole-slide multiresolution gigapixel (100,000 pixels by 100,000 pixels) images with only global data labels. Different steps are involved in building the classifier. First, WSI is cut up into small 112 by 112 μm squares (224 pixels x 224 pixels), called "tiles." Then, these tiles are fed into the CHOWDER network architecture which assigns, through an iterative learning process, a "transitional score" to each tile associated with its predictive contribution to classify the case as TM. Finally, the network selects the tiles of each WSI most relevant to predict the tumor subgroup. We give a detailed description of the different algorithm steps, as previously described[36] in the extended method section. To account for biases, the groups were evenly balanced with respect to the current histologic classification (see Fig. 2).

Statistical Analysis

The overall agreement was calculated according to the recommendation of Landis et al.[37] and was assessed using weighted chance corrected agreement with a linear weighting. For simple Kappa (k) coefficient calculation, the diagnosis was ordered as follows: (1) non-TM, and (2) TM. Univariate analysis was performed for age, sex, asbestos exposure, histologic subtypes and results of *BAP1* and *CDKN2A*(p16) homozygous deletion. Finally, the survival duration in months was calculated from the date of the initial pathologic diagnosis until the date of death according to Kaplan-Meier methodology. Groups were compared using the log rank test. Multivariate analysis Cox proportional hazards regression adjusted for age included the factors affecting survival in univariate analysis ($p < 0.20$). Hazard ratios and 95% confidence intervals were computed. Data were updated on June 30, 2018. Chisquare test and Fisher's exact bilateral test were used for comparisons between categorical variables. Statistical calculations were performed using SAS 9.4 from SAS Institute Inc. The contribution of RNASeq and deep learning in the recognition of this particular pattern of mesothelioma was also analyzed.

Results

Patient Demographics

The 49 patients had a mean age of 72 years (range, 53–88); 78% were male, and 81% had asbestos exposure history. Clinical presentations include dyspnea (73%), loss of performance status (80%), thoracic pain (83%), and pleural effusion (98%). Observations on computed tomography include pleural thickening (95%), a dominant localized pleural mass (38%), and pleural hyaline plaques (47%) (Table 2).

Interobserver Agreement

The 16 panelists recorded a total of 784 diagnoses on the 49 cases. They diagnosed the presence of a TM component in 51% of opinions (400 of 784) (Table 3). For the remaining 49%, the reviewers classified the lesion as pure epithelioid in 53% (204 of 384), pure sarcomatoid in 33% (127 of 384), and biphasic in 14% (53 of 384). The overall interobserver correlation on the identification of a TM component either diffuse or focal was moderate (k = 0.42). The interobserver agreement ranged from poor k (0.10) to excellent k (0.86) (Fig. 3). The distribution of panel diagnosis for each case is highlighted in Figure 4.

To evaluate the recognition of the presence of a diffuse or focal TM component and the structural criteria for identifying them, the 49 cases were separated into two groups on the basis of the diagnosis made by the reviewers: a TM group with the samples diagnosed as TM by expert consensus, and a non-TM group with the lesion classified as EM, BM, or SM. The presence of a diffuse TM pattern was observed in 6% (24 of 384) of the non-TM cases as compared with 77% (309 of 400) of the TM group ($p < 0.0001$). A focal TM component was diagnosed in 49% (190 of 384) of the non-TM group and in 70% (280 of 400) of the TM group ($p < 0.0001$) (Table 3).

Criteria Used to Identify the TM Pattern

For the identification of the TM component, the reviewer’s diagnosis was based on lack of frank sarcomatous features in 78% (Fig. 5A) and large round nuclei with prominent nucleoli 87% (Fig. 5B and Table 4).

At cellular level, the presence of sheet-like cell growth was observed in 83% (246 of 296) of non-TM and 90% (356 of 397) of TM ($p = 0.01$). The presence of cohesive cells was more of a feature of the TM group (83%, 330 of 398) than the non-TM group (77%, 227 of 296) ($p = 0.05$) (Table 5). The well-defined cell borders criterion was met in 55% (163 of 296) of non-TM and in 88% (351 of 400) of TM ($p < 0.0001$). The epithelioid shape with moderate to abundant cytoplasm was seen in 62% (210 of 292) of non-TM and 89% (356 of 400) of TM ($p < 0.0001$). The presence of elongated plump cells (with moderate to abundant cytoplasm losing their epithelioid structure but not overtly spindle-shaped) was identified in 80% (234 of 296) of non-TM and 94% (374 of 400) of TM ($p < 0.0001$.) Finally, the criterion of tapering cells was observed in 76% (165 of 218) of non-TM and 95% (380 of 400) of TM ($p < 0.0001$) (Table 5). The reviewers confirmed the presence of a lack of frank sarcomatous features in the recognition of the TM pattern in 78% of the cases (278 of 357).

The characteristics of aggressiveness used in this study based on grading of the tumor[34] were the presence of large round nuclei with prominent nucleoli, high nuclear-cytoplasmic ratio, mitosis, and atypical mitosis (Fig. 5B). Large round nuclei with prominent nucleoli were identified in 87% (322 of 369) of the TM group; high nucleocytoplasmic ratio in 49% (180 of 368), and mitoses in 68% (234 of 344); and when mitoses were identified, atypical mitosis were reported in 66% (143 of 216) (Table 4).

Reticulin Staining

Reticulin staining highlighted the outline of each cell in TM and SM, whereas in the epithelioid type, reticulin surrounded clusters of cells. A strong reticulin pattern of banding individual cells indicated SM; whereas a pattern of thin, delicate pattern around individual cells indicated TM, compared with a large cluster of epithelioid cells delineated by reticulin staining in EM type (Fig. 6A–C).

Survival of the TM Group

The median survival time of 44 patients with TM was 6.7 months. Five patients were excluded in survival analysis because of the presence of less than 50% of identified TM components by the reviewers (Fig. 4, case numbers 33, 41, 32, 28, 23). Overall survival was 15% at 1 year (95% confidence intervals), 5% at 2 years, and 0% at 5 years. We initially compared the overall survival with the large cohort of EM in MESOBANK, including 6154 patients with EM. The TM group has a median survival of 6.7 months, which was significantly different ($p < 0.0001$) from EM, which has a median survival of 14.7 months (59% at 1 year, 28% at 2 years, 5% at 5 years), and BM, which has a median survival of 8.8 months (38% at 1 year, 9% at 2 years, and 1% at 5 years). However, this is not significantly different from the median survival of SM (4.8 mo, 17% at 1 year, 6% at 2 years, and 1% at 5 years) (Fig. 7A). We also evaluated the median survival of TM compared with the more aggressive patterns of the solid EM type versus nonsolid subtypes. There was still a significant difference ($p < 0.0001$) between both types, with a median survival of 16.0 months (63% survival at 1 year, 31% at 2 years, and 4% at 5 years) for the nonsolid EM subtype, and 12.7 months (52% at 1 year, 21% at 2 year, and 2% at 5 years) for solid EM subtype (Fig. 7B). Interestingly, the survival curve of the transitional type was significantly different from the survival curve of the BM, but not significantly different from the overall survival curve of SM. To support the theory of TM component being a poor prognostic indicator, we have evaluated the survival curve between only two components of mesothelioma: focal versus diffuse. There was no significant difference between both of them (Fig. 7C). We then also compared the TM curve to the very aggressive pleomorphic variant of MM. There was no significant difference between the survival curve of TM and the pleomorphic variant of MM ($P = 0.13$) (Fig. 7D).

Molecular Bio-Signatures of the TM Pattern

BAP1 loss was observed in 44% (15 of 34) of cases with TM pattern, in 65% (558 of 856) of EM, in 50% (48 of 95) of BM, and 21% (13 of 62) of SM. The loss of *BAP1* was less frequent in TM than in EM and BM ($p <0.0001$) but was higher than in SM ($p < 0.0001$). p16 Loss was observed in 92% (29 of 34) of the TM cases, in 56% (563 of 1010) of EM cases, 73% (94 of 129) of BM, and in 75% in SM (78 of 104) ($p < 0.0001$). There was also

a significant difference between the four types of mesothelioma, with a significant gradient for the presence of homozygous p16 deletion being higher in TM 73% (16 of 22), followed by 67% (65 of 97) in BM, 63% (58 of 92) in SM, and only 46% (118 of 256) in EM (p = 0.0003) (Table 6).

Unsupervised hierarchical clustering revealed that TM had grouped (at the exception of two samples clustering within the SM), and that they were much closer to SM than to EM (Fig. 8A and Supplementary Fig. 1*A*). We found 260 genes significantly different between TM and EM (supplementary Fig. 1*B*). No gene was found significantly and differentially expressed between TM and SM (Supplementary Fig. 1*B*), indicating the close transcriptional relationship between TM and SM. There was a very strong enrichment of genes involved in the cell cycle progression (Fig. 8*C*) when we explored the genes up- and down-regulated in TM. To confirm that each TM tumor presented this enrichment, a single sample gene set analysis was performed using the hallmark G2/M Geneset from the Broad Institute. As shown in Figure 8*D*, all TM presented a normalized enrichment score far superior to the ones of the EM and roughly similar to those of the SM.

Altogether, these results indicate that RNASeq unsupervised clustering analyses can group most of the TMs, and also that TM shares the transcriptional profile and the aggressiveness pattern of SM.

AI: Deep Learning Analysis

The CHOWDER model achieved 94% accuracy in cross-validation (fourfold) and an area under the curve of 0.96. This repeated cross-validation (training on three-quarters of the data set, testing on the last quarter) is designed to avoid our performance being caused by overfitting, and attest the real ability of the algorithm to detect transitional patterns (see Annex 1). Furthermore, the interpretability design of CHOWDER allowed us to extract the tiles most associated with the prediction of the transitional subgroup.

A pathologist (FGS) reviewed the top five tiles mostly associated with the transitional prediction of the top two cases for each fold (Fig. 9). In seven of eight cases, the model was able to precisely identify tiles with a transitional pattern and correctly classify the tumors. This shows that the model can make the correct classification on the basis of histologic features of interests without any local annotations.

Discussion

To our knowledge, this is the first description of a large series of TM evaluated by a group of panelists from the French and IMPs with an evaluation of structural criteria, immunohistochemical expression, FISH analysis, and transcriptomic profile. This study on the TM pattern of mesothelioma confirms the use of specific histological criteria to identify its presence, regarding this to have a major impact as a poor survival prognostic indicator for therapeutic decision making. It also reports that MPMs with a TM pattern reveal rates of *BAP1* loss and *CDKN2A* P16 deletion closer to the SM type. This article also reports, for the first time, that deep learning can identify complex mesothelial cellular structure with a high level of accuracy.

Interobserver Agreement on the Transitional Pattern

Whereas a Kappa value of 0.42 is moderate, panelists documented a TM pattern in only 51% of the 791 individual diagnosis on the 49 cases (cases initially diagnosed as having a TM component by MESOPATH pathologists). Discrimination was better when the TM pattern was scored as diffuse (78% of the TM group versus 8% of the non-TM group) rather than focal (74% of the TM group versus 62% of the non-TM group), indicating that a certain percentage of the pattern may allow for more accurate interobserver discrimination. Of note, cases diagnosed as EM in 53%, BM in 14%, and SM in 33% of the non-TM group were considered to have focal TM tiles by deep learning and by transcriptomic profiling with a very strong enrichment of genes involved in the cell cycle progression. One explanation for the level of interobserver agreement of the three conventional subtypes is that 2015 WHO classification does not specify whether the TM subtype should be regarded as epithelial or sarcomatous; and so when this pattern was present, reviewers were uncertain about how this new pattern should be used to classify cases in the trichotomous scheme. This remains an issue that needs to be resolved in future classifications.

Molecular data in this study confirmed that MPM is a very heterogeneous disease. This heterogeneity has been previously documented, first by the large, deep sequencing studies by Bueno et al.[38] and Hmeljak et al.,[13] from The Cancer Genome Atlas Program group, and then by Alcala et al.[39] from the French MESOMICS project. In this latter study, the authors reported the existence of molecular alterations reflecting intratumor heterogeneity and of aggressiveness in the three conventional MPM types. Our data reveal a closer association with SM than EM, even in cases with only focal TM pattern, which may have relevance in deciding any potential cutoff for the significance of a TM pattern being present. The clustering of our analysis was rather homogeneous because of a similar proportion of differentiated cells in the selected area of TM component, except for two samples that clustered with the SM, probably because of a prominent sarcomatoid component.

Modalities to Identify a Transitional Component

The panelists were in major agreement on the structural criteria initially described by the group for the identification of TM characteristics. A major agreement was observed on three criteria: (1) lack of frankly sarcomatous features (78%, 278 of 357); presence of sheet-like cell growth (90%, 356 of 397); and presence of cohesive cells (83%, 330 of 398). At the cytologic level, the panelists recognized the following criteria of great value in the identification of TM pattern: (1) well-defined cell borders (88%, 351 of 400), epithelioid-like shape with moderate to abundant cytoplasm (88%, 351 of 400), plump cells (94%, 374 of 400); and elongated or tapering cells (95%, 380 of 400).

Even if the reviewers observed an absence of frank sarcomatous component, they recognized high-grade features with the presence of large ovoid nuclei with prominent nucleoli in 82% and the presence of mitosis in 73% (415 of 572).

The TM component is ambiguous and raised several differential diagnoses between sarcomatoid carcinoma, nonspindled melanoma, and sarcoma routinely diagnosed by a

battery of well-known immunohistochemical markers or RNASeq. The separation of EM versus SM is more challenging.

The use of reticulin was well-known in the diagnosis of carcinoma versus sarcoma to separate epithelial from sarcomatous cells. Our study also reported that reticulin staining is useful for the separation between epithelioid and nonepithelioid (TM or SM) type, nicely highlighted by the thin delimitation of each cell (Fig. 5A). One explanation for this phenomenon may come from the study of Kang et al.,[10] who reported that glycosaminoglycans may play an important role in the formation of fibrous, long-spacing collagen fibrils in MPM. They are present in EM and BM owing to the high concentration of hyaluronic acid–embedding microvilli, and not in SM. Therefore, the reticulin staining seems to be a very simple and useful tool for the separation of TM from EM, but not from SM.

At the Molecular Level

The molecular analysis of this series revealed that *BAP1* loss, known to be more often observed in EM as an indicator of a better prognosis, is less often observed in TM; the percentage of *BAP1* loss in TM is very close to BM but higher than in SM. Similarly, HD p16, an indicator of a worse prognosis in MPM, is significantly more often observed in TM (73%) than in the other types of MPM, with a descending gradient to EM observed only in 46% conferring a characteristic signature of prognosis in TM. In addition, transcriptomic analysis (Fig. 9*A*) revealed that TM (orange) clustered together with the sarcomatoid (red) but away from the EM (blue) and are mainly driven by genes of aggressiveness of the cell cycle (Fig. 8*C*).

Is the TM Pattern a Model of Epithelial-Mesenchymal Transition?

Despite advances in molecular characterization of MPM,[13,38,39] little is known on the various genetic, phenotypic and microenvironmental events responsible for intratumor heterogeneity and the exact place and role of epithelial-mesenchymal transition (EMT) in mesothelioma progression. The EMT is usually characterized by the dedifferentiation from an epithelial to a mesenchymal phenotype, with a specific immunophenotype profile showing a decrease of expression in vimentin from mesenchymal to epithelial and decrease of expression of E-cadherin to N-cadherin. These data are arguments in favor of distinct molecular events driving changes from epithelial to mesenchymal phenotype associated with dysregulation of cell-cell or cell-matrix attachment responsible for the loss of adhesion, invasion, and dissemination. We have observed a tendency (but without being significant) of TM having an expression of EMT-involved genes as high as SM but higher than EM, similar to what we observed for the cell-cycle genes. Nevertheless, from the data, we acquired tumor-wide (2500 RNASeq of ~150 tumor subtypes) we do not observe a correlation (nor anticorrelation) between EMT and cell-cycle scores ($r^2 = 0.00661$). From these bioinformatics analyses, expression of genes involved in EMT (at least those present in the broad MSigDB EMT hallmark) seem to be independent of the cell cycle. Nevertheless, we wanted to emphasize that although it makes sense to believe that the genes involved in EMT have different expression levels in EM and SM, we observed some EM samples with high expression of these genes, which was also indirectly revealed by the absence of EMT

in gene set enrichment analysis. Our study reported that EMT does not discriminate between SM, EM, and TM (Fig. 7D).

In conclusion, the interobserver agreement among practicing thoracic pathologists suggests that this pattern can be identified with sufficient reproducibility for diagnostic usage; although, further work is required to improve this level. It also suggests that a TM pattern behaves more like an SM type, with closer molecular signature to SM, and usually shows high-grade nuclear features that may provide important biological insights, which could be used for the development of therapeutic targets.

Finally, deep learning may assist pathologists in the identification of these histologically complex cellular structures.

Taken together, for the first time, our results confirmed that TM pattern should be considered as an aggressive subtype of MM, characterized by distinct structural criteria, reticulin pattern, and transcriptomic profile, and should be classified as a non-EM (at minimum as a subgroup of SM) and not as an EM variant of mesothelioma.

Supplementary Material

Refer to Web version on PubMed Central for supplementary material.

Authors

Francoise Galateau Salle, MD[a,*], Nolwenn Le Stang, PhD[a], Franck Tirode, PhD[b], Pierre Courtiol, MSc[c], Andrew G. Nicholson, FRCPath[d], Ming-Sound Tsao, MD[e], Henry D. Tazelaar, MD[f], Andrew Churg, MD[g], Sanja Dacic, MD, PhD[h], Victor Roggli, MD[i], Daniel Pissaloux, PhD[j], Charles Maussion, MSc[c], Matahi Moarii, PhD[c], Mary Beth Beasley, MD[k], Hugues Begueret, MD[l], David B. Chapel, MD, PhD[m], Marie Christine Copin, MD, PhD[n], Allen R. Gibbs, M.B.B.S., FRCPath[o], Sonja Klebe, MD, PhD, FRCPA[p], Sylvie Lantuejoul, MD, PhD[a], Kazuki Nabeshima, MD, PhD[q], Jean-Michel Vignaud, MD, PhD[r], Richard Attanoos, M.B.B.S., FRCPATH[o], Luka Brcic, MD, PhD[s], Frederique Capron, MD, PhD[t], Lucian R. Chirieac, MD[u], Francesca Damiola, PhD[a], Ruth Sequeiros, MD[a], Aurélie Cazes, MD, PhD[a,v], Diane Damotte, MD, PhD[a,w], Armelle Foulet, MD[a,x], Sophie Giusiano-Courcambeck, MD[a,y], Kenzo Hiroshima, MD, PhD[z], Veronique Hofman, MD, PhD[a,f,aa], Aliya N. Husain, MD, PhD[m], Keith Kerr, FRCPath, PhD[bb], Alberto Marchevsky, MD[cc], Severine Paindavoine, MSc[b], Jean Michel Picquenot, MD[a,dd], Isabelle Rouquette, MD[a,ee], Christine Sagan, MD[a,ff], Jennifer Sauter, MD[gg], Francoise Thivolet, MD, PhD[a,hh], Marie Brevet, MD, PhD[a,hh], Philippe Rouvier, MD[t], William D. Travis, MD[gg], Gaetane Planchard, MD[a,ii], Birgit Weynand, MD, PhD[jj], Thomas Clozel, PhD[c], Gilles Wainrib, PhD[c], Lynnette Fernandez-Cuesta, PhD[kk], Jean-Claude Pairon, MD, PhD[ll], Valerie Rusch, MD[mm], Nicolas Girard, MD, PhD[nn]

Affiliations

[a]MESOPATH, MESONAT, MESOBANK Department of BioPathology Centre Leon Berard, Lyon, France

[b]University Claude Bernard Lyon, INSERM, CNRS, Research Cancer Center of Lyon, Centre Léon Bérard, Lyon, France

[c]OWKIN Paris, France

[d]Department of Histopathology, Royal Brompton and Harefield NHS Foundation Trust and National Heart and Lung Institute, Imperial College, London, United Kingdom

[e]University Health Network, Princess Margaret Cancer Centre and University of Toronto, Department of Laboratory Medicine and Pathobiology, Toronto, Ontario, Canada

[f]Mayo Clinic, Scottsdale, Arizona

[g]Columbia University and Department of Pathology Vancouver, Canada

[h]FISH and Developmental Laboratory at the University of Pittsburgh Medical Center, Pittsburgh, Pennsylvania

[i]Duke University Medical Center, Department of Pathology, Durham, North Carolina

[j]Department of BioPathology-FISH Laboratory, Centre Leon Berard Lyon, France

[k]Mount-Sinai Medical Center, Department of Pathology, New York, New York

[l]CHU Bordeaux, Haut Leveque Hospital, Department of Pathology, Bordeaux, France

[m]University of Chicago, Department of Pathology, Chicago, Illinois

[n]University. Lille-CHU, Department of Pathology, Lille, France

[o]University of Wales, Department of Cellular Pathology, Cardiff, United Kingdom

[p]Department of Anatomical Pathology, Flinders University, Adelaide, Australia

[q]Department of Pathology, Fukuoka University School of Medicine and Hospital, Fukuoka, Japan

[r]CHU Nancy, INSERM, University of Lorraine, Lorraine, France

[s]Department of Pathology, Graz, Austria

[t]CHU Pitié Salpétrière Paris, Department of Pathology, Paris, France

[u]Brigham and Women’s Hospital, Boston, Massachusetts

[v]CHU Bichat Department of Pathology, University Paris VII, Paris, France

[w]CHU Cochin-Hotel Dieu, Department of Pathology, Paris, France

[x]CH Le Mans, Department of Pathology, Pays de la Loire, France

[y]CHU Hospital Nord, Marseille, University Aix-Marseille, Marseille, France

[z]Tokyo Women’s Medical University, Department of Pathology, Tokyo, Japan

[aa]CHU Nice, Department of Clinical and Experimental Pathology (LPCE), Nice, France

[bb]Aberdeen Royal Infirmary, Department of Pathology, Aberdeen, Scotland

[cc]Scotland Cedars-Sinai Medical Center, Department of Pathology, Los Angeles, California

[dd]Department of Pathology, Henri Becquerel Centre, Rouen, France

[ee]IUCT-Oncopôle, Department of Pathology, Toulouse, France

[ff]CHU Nantes, INSERM, Thorax Institute, Hôpital Laënnec CHU Nantes, Nantes, France

[gg]Memorial Sloan Kettering Cancer Center, Department of Pathology, New York, New York

[hh]Hospices Civils, East Hospital Group, Department of Pathology, Lyon, France

[ii]Department of Pathology, CHU Caen, Caen, France

[jj]UZ Leuven, Department of Pathology, Leuven, Belgium

[kk]Genetic Cancer Susceptibility Group International Agency for Research on Cancer World Health Organization, Lyon, France

[ll]INSERM, UPEC, Faculty of Medicine and CHI Creteil, Professional Pathologies and Environment Department, IST-PE, Creteil, France

[mm]Memorial Sloan Kettering Cancer Center, Department of Thoracic Surgery, New York, New York

[nn]Department of Thoracic Oncology Institute Curie Paris, France and European Reference Network EURACAN, Centre Leon Berard, France

Acknowledgments

This work and the International Mesothelioma Panel were supported by The National Cancer Institute core grant and Santé Publique France since 1998. The work of Dr. Rusch and Dr. Travis is supported in part by National Institutes of Health/National Cancer Institute Cancer Center Support Grant (grant number P30 CA008748). The authors thank all the experts of the MESOPATH National Reference Center who have supported the MESOBANK with materials and participated in the procedure of certification for all cases included in the data analysis, including I. Abdalsamad, E. Brambilla, C. Danel, A. de Lajartre, L. Garbe, O. Groussard, and R. Loire. The authors also thank the participants of the International Mesothelioma Panel, K. Butnor, A. Moreira, and A. Roden for the great discussion and comments; Pr Jean Yves Blay for his support; French National Cancer Institute and the National Health Institute (SpF) for their financial support to the MESOPATH National Reference Center; and an anonymous donor for unrestricted grants.

Disclosure:

Mr. Courtiol, Mr. Maussion, Dr. Moarii, Dr. Clozel, and Dr. Wainrib have a patent pending for systems and methods for mesothelioma feature detection and enhanced prognosis. Dr. Roggli consults with plaintiff and defense attorneys in asbestos litigation. Drs. Beasley and Gibbs report doing medicolegal work concerning mesothelioma causation. Dr. Klebe reports preparing medicolegal reports on diagnosis and causation of mesothelioma. Dr. Attanoos reports being retained by claimants and defendants and on a joint basis in asbestos litigation. Dr. Brcic reports receiving grants, personal fees, and nonfinancial support from AstraZeneca, MSD, and Roche, and nonfinancial support from Pfizer outside of the submitted work. Dr. Chirieac reports receiving personal fees from doing medicolegal work related to mesothelioma outside of the submitted work. Dr. Rusch reports receiving grants from Genelux, Inc. and Genentech; other funding from Intuitive Surgical and National Institutes of Health-Coordinating Center for Clinical

Trials; and nonfinancial support from Mesothelioma and Radical Surgery 2 Trial Data and Safety Monitoring Committee outside of the submitted work. The remaining authors declare no conflict of interest.

References

1. Bray F, Ferlay J, Soerjomataram I, Siegel RL, Torre LA, Jemal A. Global cancer statistics 2018: GLOBOCAN estimates of incidence and mortality worldwide for 36 cancers in 185 countries. CA Cancer J Clin. 2018;68:394–424. [PubMed: 30207593]
2. Opitz I, Friess M, Kestenholz P, et al. A new prognostic score supporting treatment allocation for multimodality therapy for malignant pleural mesothelioma: a review of 12 years' experience. J Thorac Oncol. 2015;10:1634–1641. [PubMed: 26317916]
3. Hasegawa S, Okada M, Tanaka F, et al. Trimodality strategy for treating malignant pleural mesothelioma: results of feasibility study of induction pemetrexed plus cisplatin followed by extrapleural pneumonectomy and postoperative hemithoracic radiation (Japan Mesothelioma Interest Group 0601 Trial). Int J Clin Oncol. 2016;21:523–530. [PubMed: 26577445]
4. Tsao AS, Lindwasser OW, Adjei AA, et al. Current and future management of malignant mesothelioma: a consensus report from the National Cancer Institute Thoracic Malignancy Steering Committee, International Association for the Study of Lung Cancer, and Mesothelioma Applied Research Foundation. J Thorac Oncol. 2018;13:1655–1667. [PubMed: 30266660]
5. McCambridge AJ, Napolitano A, Mansfield AS, et al. Progress in the management of malignant pleural mesothelioma in 2017. J Thorac Oncol. 2018;13:606–623. [PubMed: 29524617]
6. Stahel RA, Riesterer O, Xyrafas A, et al. Neoadjuvant chemotherapy and extrapleural pneumonectomy of malignant pleural mesothelioma with or without hemithoracic radiotherapy (SAKK 17/04): a randomised, international, multicentre phase 2 trial. Lancet Oncol. 2015;16:1651–1658. [PubMed: 26538423]
7. Tartarone A, Lerose R, Aieta M. Is there a role for immunotherapy in malignant pleural mesothelioma? Med Oncol. 2018;35:98. [PubMed: 29845408]
8. Scherpereel A, Mazieres J, Greillier L, et al. Nivolumab or nivolumab plus ipilimumab in patients with relapsed malignant pleural mesothelioma (IFCT-1501 MAPS2): a multicentre, open-label, randomised, non-comparative, phase 2 trial [published correction appears in Lancet Oncol. 2019;20:e132]. Lancet Oncol. 2019;20:239–253. [PubMed: 30660609]
9. Galateau Salle F, Le Stang N, Nicholson AG, et al. New insights on diagnostic reproducibility of biphasic mesotheliomas: a multi-institutional evaluation by the International Mesothelioma Panel from the MESOPATH reference center. J Thorac Oncol. 2018;13:1189–1203. [PubMed: 29723687]
10. Kang D, Kunugi S, Masuda Y, Ishizaki M, Koizumi K, Fukuda Y. Ultrastructural and immunohistochemical analysis of fibrous long-spacing collagen fibrils in malignant mesothelioma. Ultrastruct Pathol. 2009;33:52–60. [PubMed: 19274581]
11. Travis WD, Brambilla E, Burke AP, Marx A, Nicholson AG. WHO Classification of Tumors of the Lung, Pleura, Thymus and Heart. Lyon France: IARC Press; 2015.
12. Galateau-Salle F, Churg A, Roggli V, Travis WD, World Health Organization Committee for Tumors of the Pleura. The 2015 World Health Organization classification of tumors of the pleura: advances since the 2004 classification. J Thorac Oncol. 2016; Feb;11:142–154. [PubMed: 26811225]
13. Hmeljak J, Sanchez-Vega F, Hoadley KA, et al. Integrative molecular characterization of malignant pleural mesothelioma. Cancer Discov. 2018;8:1548–1565. [PubMed: 30322867]
14. Mc Gregor SM, Dunning R, Hyjek E, Vigneswaran W, Husain AN, Krausz T. BAP1 facilitates diagnostic objectivity, classification, and prognostication in malignant pleural mesothelioma. Hum Pathol. 2015;46:1670–1678. [PubMed: 26376834]
15. Hwang HC, Pyott S, Rodriguez S, et al. BAP1 immunohistochemistry and p16 FISH in the diagnosis of sarcomatous and desmoplastic mesothelioma. Am J Surg Pathol. 2016;40:714–718. [PubMed: 26900815]
16. Tochigi N, Attanoos R, Chirieac LR, Allen TC, Cagle PT, Dacic S. p16 Deletion in sarcomatoid tumors of the lung and pleura. Arch Pathol Lab Med. 2013;137:632–636. [PubMed: 23627453]

17. Wu D, Hiroshima K, Yusa T, et al. Usefulness of p16/CDKN2A fluorescence in situ hybridization and BAP1 immunohistochemistry for the diagnosis of biphasic mesothelioma. Ann Diagn Pathol. 2017;26:31–37. [PubMed: 28038708]
18. Lesluyes T, Pérot G, Largeau MR, et al. RNA sequencing validation of the Complexity Index in SARComas prognostic signature. Eur J Cancer. 2016;57:104–111. [PubMed: 26916546]
19. Salakhutdinov R, Hinton G. An efficient learning procedure for deep Boltzmann machines. Neural Comput. 2012;24:1967–2006. [PubMed: 22509963]
20. Hinton G Deep learning-a technology with the potential to transform health care. JAMA. 2018;320:1101–1102. [PubMed: 30178065]
21. Churg A, Attanoos R, Borczuk AC, et al. Dataset for reporting of malignant mesothelioma of the pleura or peritoneum: recommendations from the International Collaboration on Cancer Reporting (ICCR). Arch Pathol Lab Med. 2016; Oct;140:1104–1110. [PubMed: 27031777]
22. Churg A, Cagle PT, Roggli VL, American Registry of Pathology, Armed Forces Institute of Pathology. Tumors of the Serosal Membranes, AFIP Atlas of Tumor Pathology. Washington, DC: American Registry of Pathology, Armed Forces Institute of Pathology; 2006.
23. Le Stang N, Burke L, Blaizot G, et al. Differential diagnosis of epithelioid malignant mesothelioma with lung and breast pleural metastasis: a systematic review compared to a standardized panel of antibodies-a new proposal that may influence pathological practice. Arch Pathol Lab Med. 2020;144:446–456. [PubMed: 31389715]
24. Husain AN, Colby TV, Ordóñez NG, et al. Guidelines for pathologic diagnosis of malignant mesothelioma 2017 update of the consensus statement from the International Mesothelioma Interest Group. Arch Pathol Lab Med. 2018;142:89–108. [PubMed: 28686500]
25. Marchevsky AM, LeStang N, Hiroshima K, et al. The differential diagnosis between pleural sarcomatoid mesothelioma and spindle cell/pleomorphic (sarcomatoid) carcinomas of the lung: evidence-based guidelines from the International Mesothelioma Panel and the MESOPATH National Reference Center. Hum Pathol. 2017;67:160–168. [PubMed: 28782639]
26. Klebe S, Brownlee NA, Mahar A, et al. Sarcomatoid mesothelioma: a clinical-pathologic correlation of 326 cases. Mod Pathol. 2010;23:470–479. [PubMed: 20081811]
27. Attanoos RL, Dojcinov SD, Webb R, Gibbs AR. Anti-mesothelial markers in sarcomatoid mesothelioma and other spindle cell neoplasms. Histopathology. 2000;37:224–231. [PubMed: 10971698]
28. Kushitani K, Takeshima Y, Amatya VJ, Furonaka O, Sakatani A, Inai K. Differential diagnosis of sarcomatoid mesothelioma from true sarcoma and sarcomatoid carcinoma using immunohistochemistry. Pathol Int. 2008;58:75–83. [PubMed: 18199156]
29. Takeshima Y, Amatya VJ, Kushitani K, Kaneko M, Inai K. Value of immunohistochemistry in the differential diagnosis of pleural sarcomatoid mesothelioma from lung sarcomatoid carcinoma. Histopathology. 2009;54:667–676. [PubMed: 19438742]
30. Berg KB, Churg A. GATA3 immunohistochemistry for distinguishing sarcomatoid and desmoplastic mesothelioma from sarcomatoid carcinoma of the lung. Am J Surg Pathol. 2017;41:1221–1225. [PubMed: 28614203]
31. Churg A, Nabeshima K, Ali G, Bruno R, Fernandez-Cuesta L, Galateau-Salle F. Highlights of the 14th international mesothelioma interest group meeting: pathologic separation of benign from malignant mesothelial proliferations and histologic/molecular analysis of malignant mesothelioma subtypes. Lung Cancer. 2018;124:95–101. [PubMed: 30268487]
32. Berg KB, Dacic S, Miller C, Cheung S, Churg A. Utility of methylthioadenosine phosphorylase compared with BAP1 immunohistochemistry, and CDKN2A and NF2 fluorescence in situ hybridization in separating reactive mesothelial proliferations from epithelioid malignant mesotheliomas. Arch Pathol Lab Med. 2018;142:1549–1553. [PubMed: 30059257]
33. Sheffield BS, Hwang HC, Lee AF, et al. BAP1 immunohistochemistry and p16 FISH to separate benign from malignant mesothelial proliferations. Am J Surg Pathol. 2015;39:977–982. [PubMed: 25634745]
34. Rosen LE, Karrison T, Ananthanarayanan V, et al. Nuclear grade and necrosis predict prognosis in malignant epithelioid pleural mesothelioma: a multi-institutional study. Mod Pathol. 2018;31:598–606. [PubMed: 29327706]

35. Bray NL, Pimentel H, Melsted P, Pachter L. Near-optimal probabilistic RNA-seq quantification. Nat Biotechnol. 2016;34:525–527. [PubMed: 27043002]

36. Courtiol P, Maussion C, Moarii M, et al. Deep learning predicts prognosis in mesothelioma independently of current histological classification and refines current prognostic criteria. Nat Med. 2019;25:1519–1525. [PubMed: 31591589]

37. Landis JR, Koch GG. The Measurement of Observer Agreement for Categorical Data. Biometrics. 1977;33:159–174. [PubMed: 843571]

38. Bueno R, Stawiski EW, Goldstein LD, et al. Comprehensive genomic analysis of malignant pleural mesothelioma identifies recurrent mutations, gene fusions and splicing alterations. Nat Genet. 2016;48:407–416. [PubMed: 26928227]

39. Alcala N, Mangiante L, Le-Stang N, et al. Redefining malignant pleural mesothelioma types as a continuum uncovers immune-vascular interactions. EBioMedicine. 2019;48:191–202. [PubMed: 31648983]

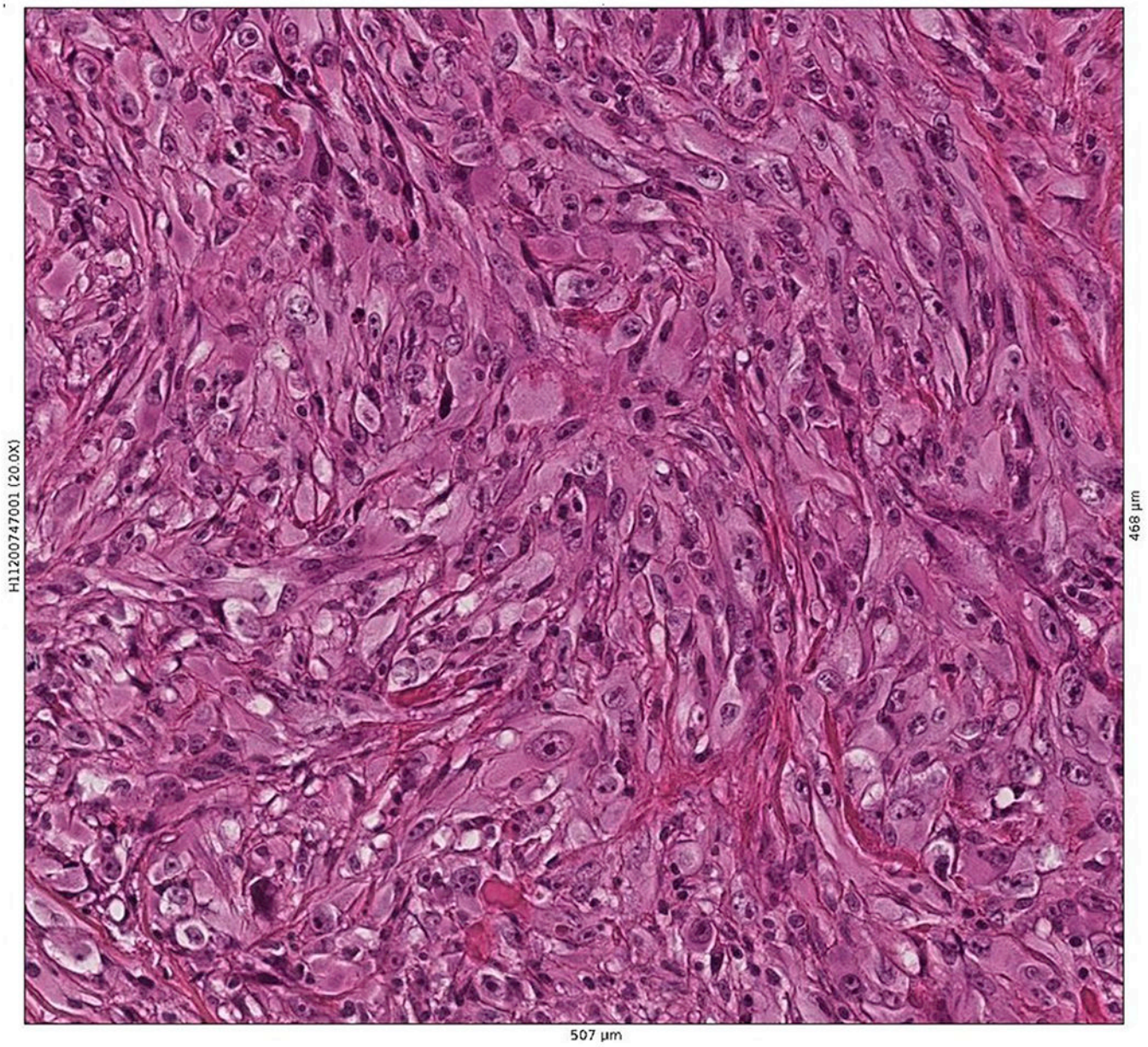

Figure 1.

Transitional pattern of cohesive, large, plump epithelioid cells with a well-defined border, high nucleocytoplasmic ratio, and prominent nucleoli.

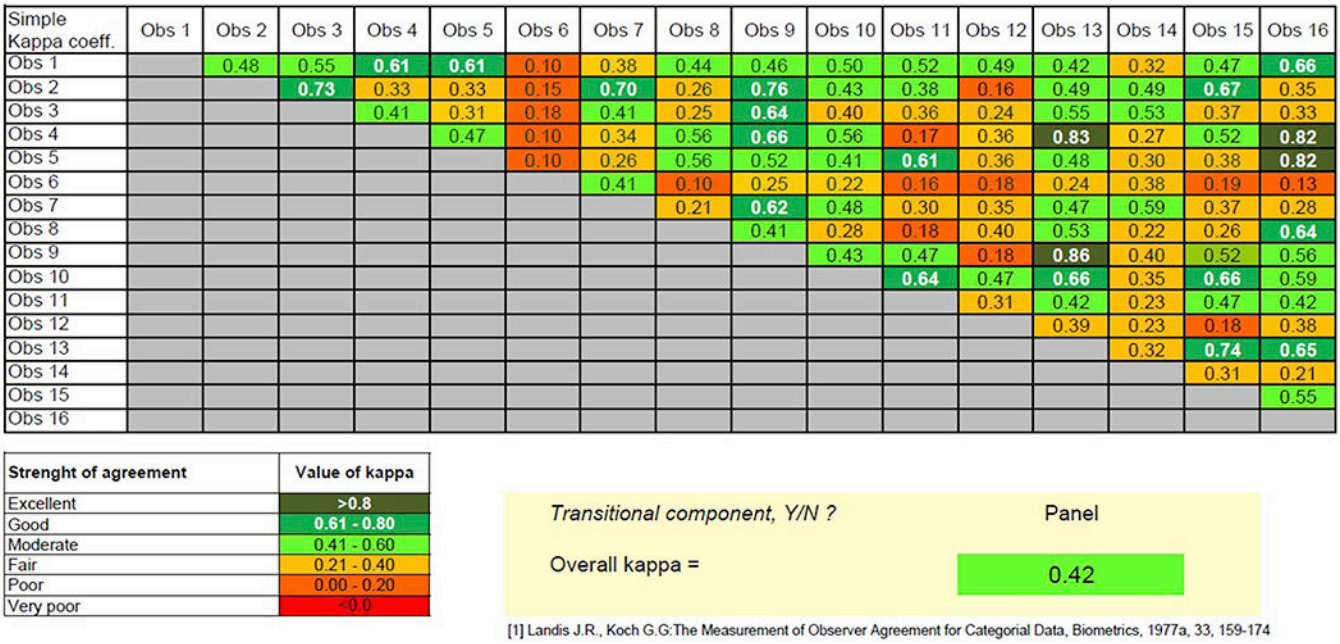

Simple Kappa coeff.	Obs 1	Obs 2	Obs 3	Obs 4	Obs 5	Obs 6	Obs 7	Obs 8	Obs 9	Obs 10	Obs 11	Obs 12	Obs 13	Obs 14	Obs 15	Obs 16
Obs 1		0.48	0.55	**0.61**	**0.61**	0.10	0.38	0.44	0.46	0.50	0.52	0.49	0.42	0.32	0.47	**0.66**
Obs 2			**0.73**	0.33	0.33	0.15	**0.70**	0.26	**0.76**	0.43	0.38	0.16	0.49	0.49	**0.67**	0.35
Obs 3				0.41	0.31	0.18	0.41	0.25	**0.64**	0.40	0.36	0.24	0.55	0.53	0.37	0.33
Obs 4					0.47	0.10	0.34	0.56	**0.66**	0.56	0.17	0.36	**0.83**	0.27	0.52	**0.82**
Obs 5						0.10	0.26	0.56	0.52	0.41	**0.61**	0.36	0.48	0.30	0.38	**0.82**
Obs 6							0.41	0.10	0.25	0.22	0.16	0.18	0.24	0.38	0.19	0.13
Obs 7								0.21	**0.62**	0.48	0.30	0.35	0.47	0.59	0.37	0.28
Obs 8									0.41	0.28	0.18	0.40	0.53	0.22	0.26	**0.64**
Obs 9										0.43	0.47	0.18	**0.86**	0.40	0.52	0.56
Obs 10											**0.64**	0.47	**0.66**	0.35	**0.66**	0.59
Obs 11												0.31	0.42	0.23	0.47	0.42
Obs 12													0.39	0.23	0.18	0.38
Obs 13														0.32	**0.74**	**0.65**
Obs 14															0.31	0.21
Obs 15																0.55
Obs 16																

Strenght of agreement	Value of kappa
Excellent	>0.8
Good	0.61 - 0.80
Moderate	0.41 - 0.60
Fair	0.21 - 0.40
Poor	0.00 - 0.20
Very poor	<0.0

Figure 2.

Distribution of Kappa scores for the recognition of the transitional mesothelioma histological component in mesothelioma.

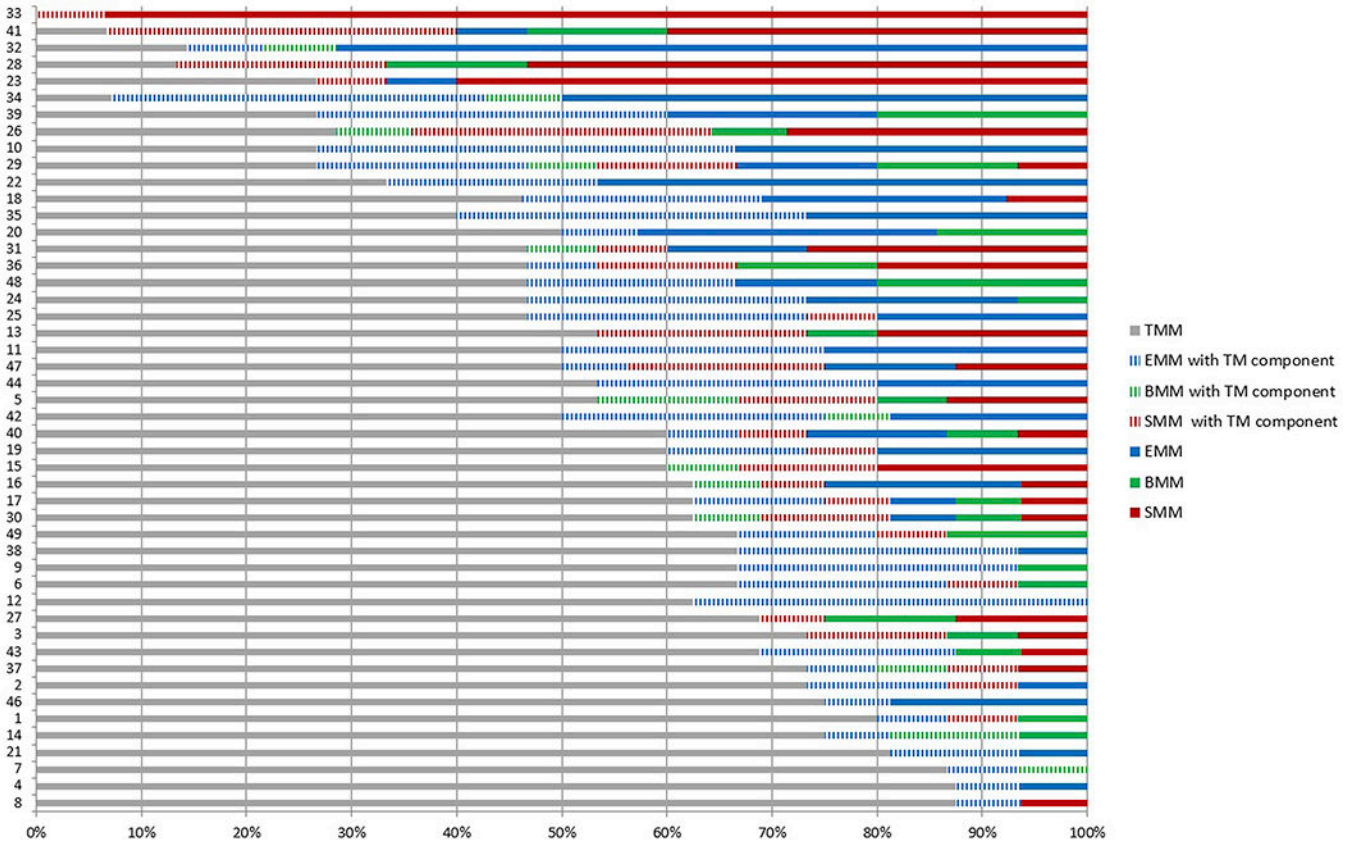

Figure 3.
Results of the interobserver agreement.

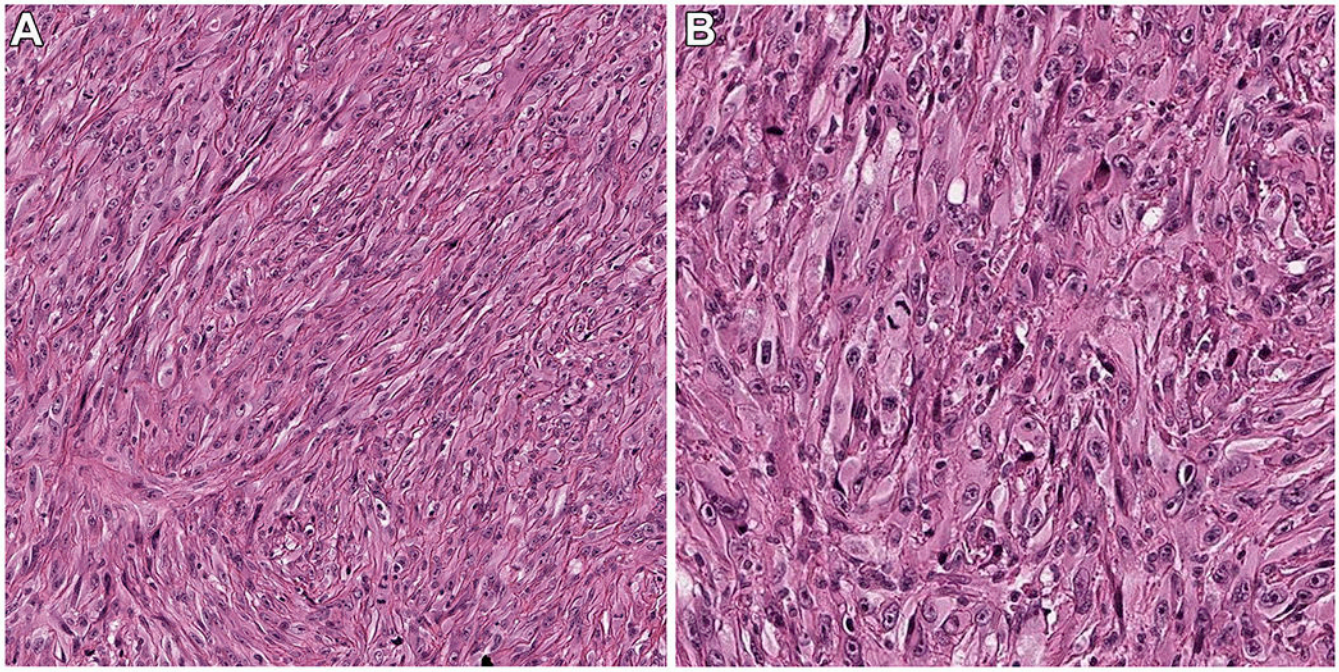

Figure 4.

Distribution of diagnosis made by the reviewers by histologic types according to the WHO 2015 classification. X-axis visualizes the percentage of diagnosis made by the reviewers for each case of the study. The Y-axis corresponds to the case number. TMM, transitional malignant mesothelioma; EMM, epithelioid malignant mesothelioma; BMM, biphasic malignant mesothelioma; SMM, sarcomatoid malignant mesothelioma.

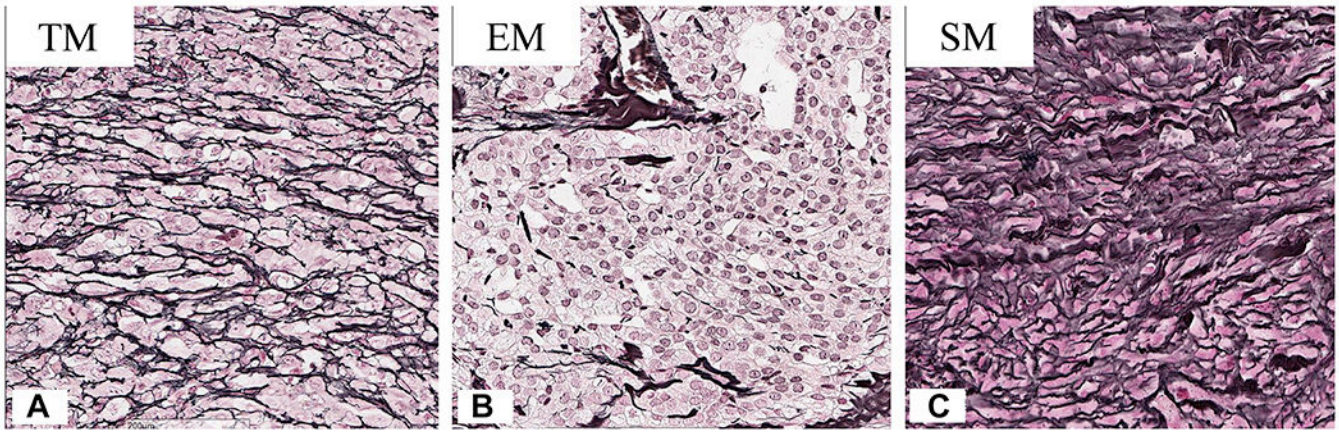

Figure 5.

(A) Image illustrating the lack of frankly sarcomatous features; *(B)* Large ovoid nuclei with prominent nucleoli and presence of mitosis).

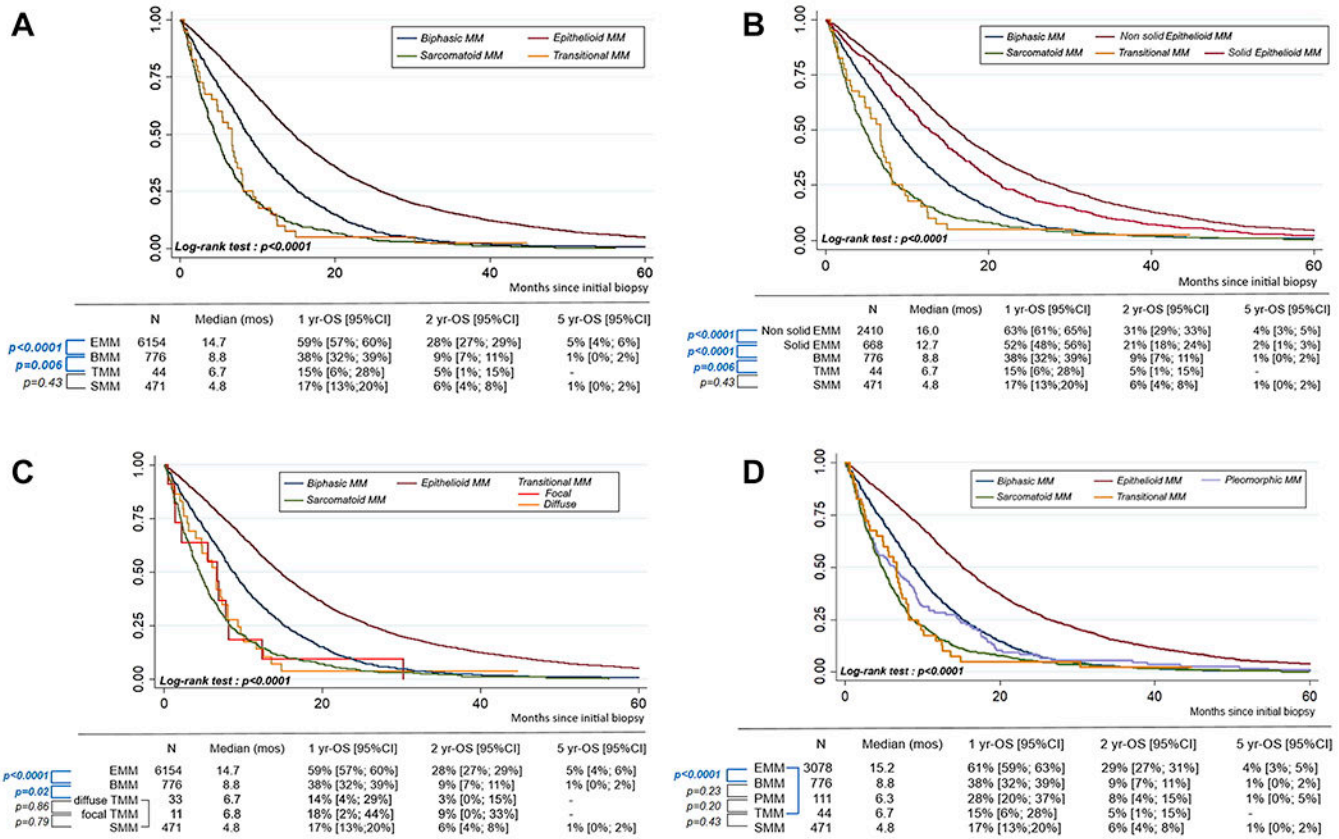

Figure 6.

(A, B, C) Reticulin staining in TM, SM, and EM showing the thin banding of individual transitional cells compared with the strong banding of individual sarcomatoid cells and the strapping of large cluster of EM cells. TM, transitional mesothelioma; EM, epithelioid mesothelioma; BM, biphasic mesothelioma; SM, sarcomatoid mesothelioma.

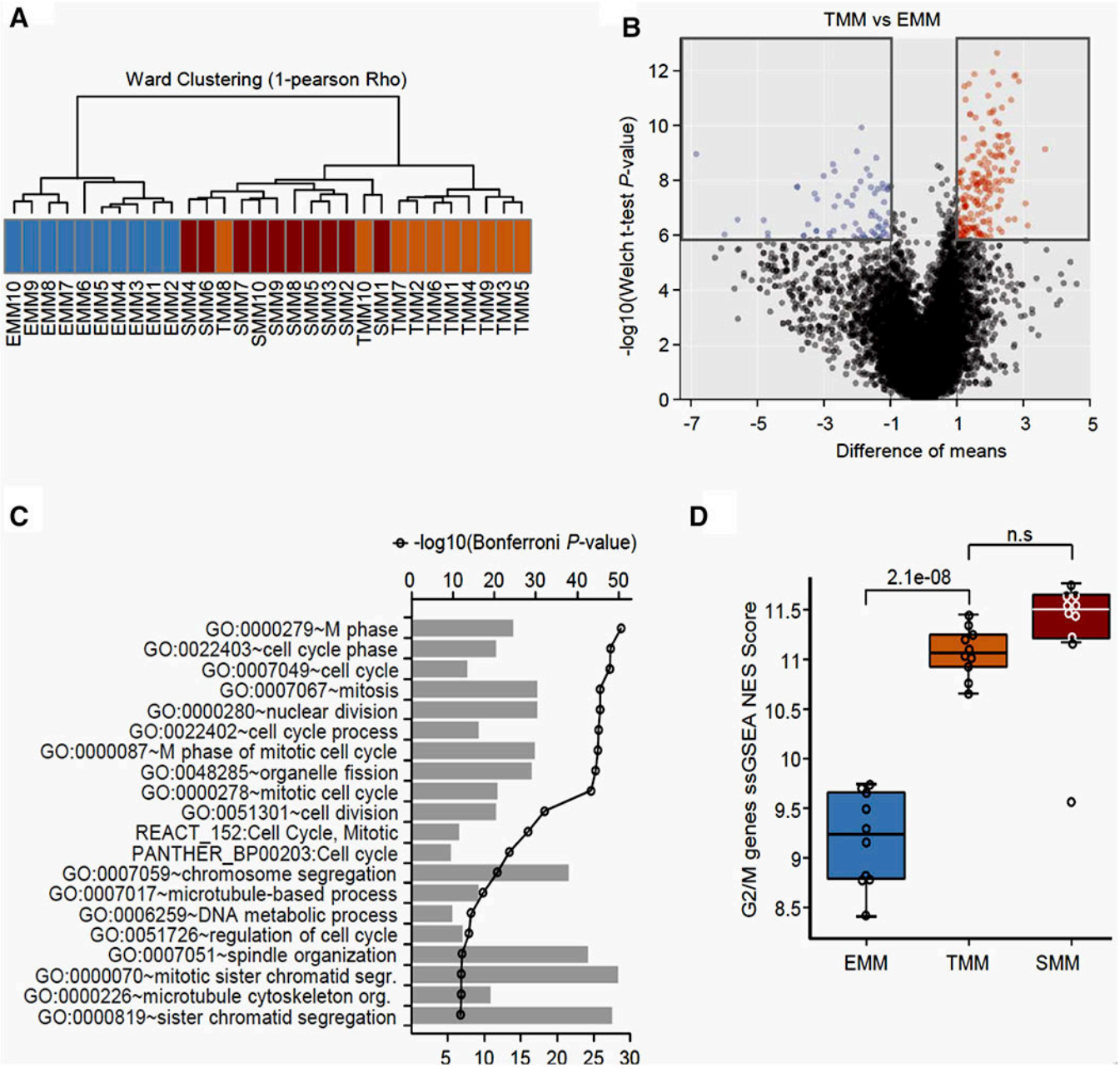

Figure 7.

(A) OS of the series of 49 TM cases compared with the epithelioid biphasic and sarcomatoid conventional histologic types from the large MESOBANK cohort; *(B)* overall survival curves of the TM series by histologic types when comparing the 49 TM cases with more aggressive patterns of epithelioid subtypes (solid and nonsolid epithelioid subtypes); *(C)* OS curves of the TM series by histologic types when comparing the 49 TM cases to epithelioid, biphasic, sarcomatoid and pleomorphic type. TM, transitional mesothelioma; OS overall survival; CI, confidence interval.

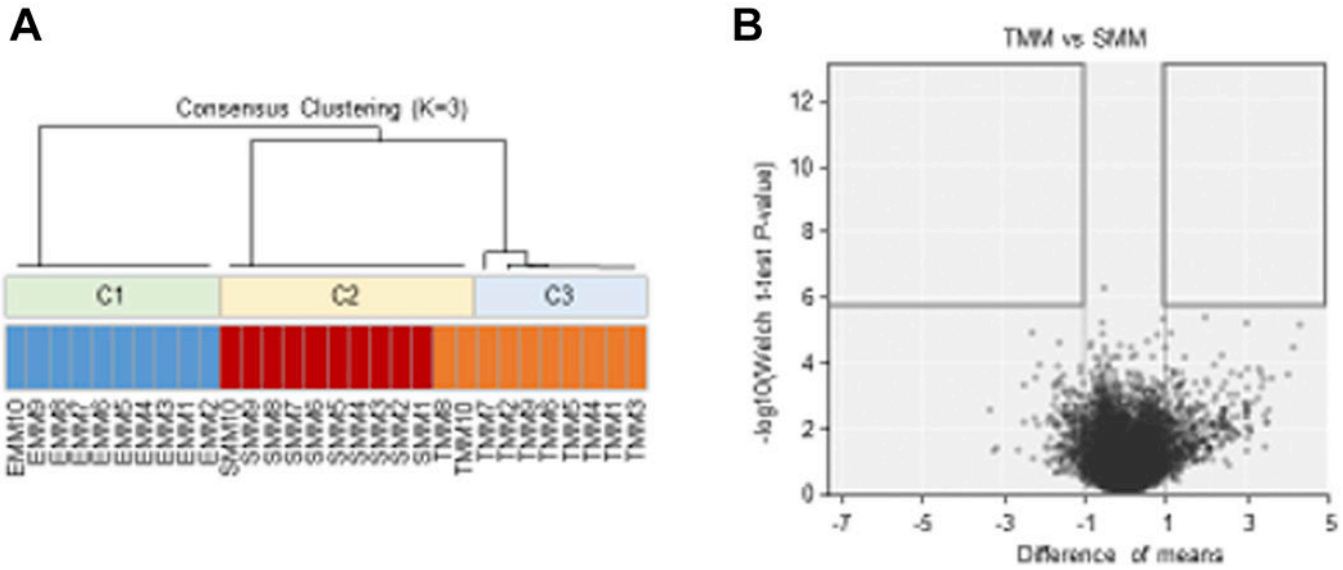

Figure 8.

RNASeq analyses of a series of 30 mesotheliomas. *(A)* Hierarchical unsupervised clustering demonstrating that transitional mesotheliomas (gray) clustered together with the sarcomatoid (black) but away from the epithelioid (white) mesotheliomas. *(B)* Volcano plot presenting the DEGs between the TMM and EMM. Gray squares delineate significant up- or down-regulated DEGs (Welch two samples test *p* value, Bonferroni corrected < 10-2 and absolute difference of mean expression >1). *(C)* Gene ontology analyses of DEGs using DAVID tool. Enrichment and Fisher exact test p value is represented for the 20 most significant pathways. *(D)* Boxplot of the NES from the single sample Gene Set Enrichment Analysis using the Hallmark_G2M_checkpoint gene set. Welch *t* test *p* values are indicated. DAVID, The Database for Annotation, Visualization and Integrated Discovery; DEGs, differentially expressed genes; EMM, epithelioid malignant mesothelioma; NES, normalized enrichment score; ns, not significant; RNASeq, RNA sequencing; TMM, transitional malignant mesothelioma.

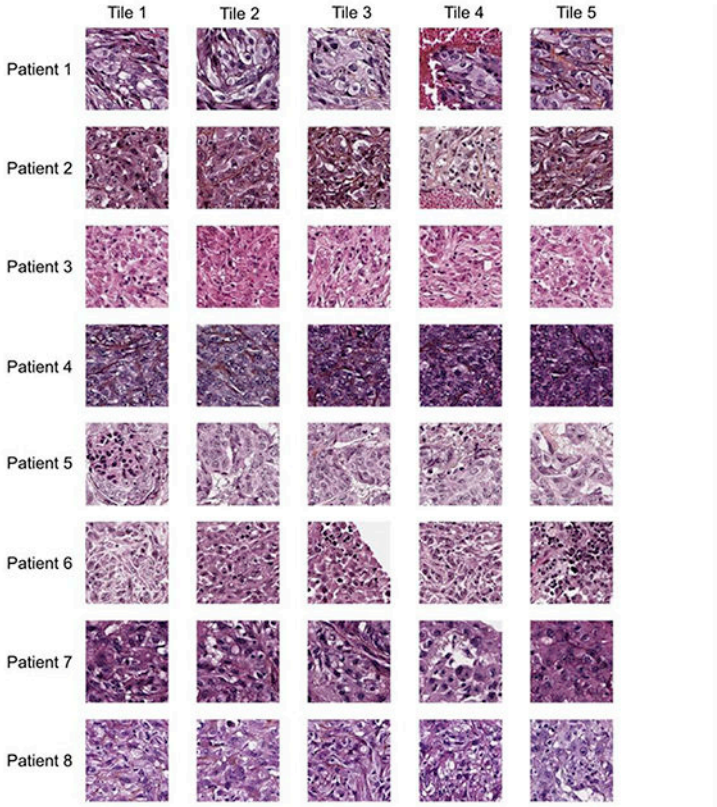

	Tile 1	Tile 2	Tile 3	Tile 4	Tile 5	Final
Patient 1	Yes	Yes	No	No	Yes	3/5
Patient 2	Yes	No	Yes	No	Yes	3/5
Patient 3	No	Yes	Yes	Yes	N/A	3/5
Patient 4	Yes	No	No	No	No	1/5
Patient 5	No	No	No	No	No	0/5
Patient 6	Yes	No	No	No	No	1/5
Patient 7	Yes	Yes	No	N/A	Yes	3/5

Figure 9.
Distribution and characterization of top five tiles for histological tiles per patient with transitional features.

Table 1.

List of Items Selected for the Review Score Sheet

Items	Possible Values
Select your diagnosis, transitional type?	No/Yes
If No,	
Other diagnosis	Epithelioid MM, Biphasic MM, Sarcomatoid MM
If Yes,	
Presence of transitional diffuse pattern	No/Yes
Presence of transitional focal pattern	No/Yes
Presence of:	
Sheet cell growth	No/Yes
Cohesive cells	No/Yes
Well-defined borders	No/Yes
Epithelial like shape with moderate to abundant cytoplasm	No/Yes
Plump cells	No/Yes
Elongated tapering cells	No/Yes
Lack of frank sarcomatous features	No/Yes
Large ovoid nuclei prominent nucleoli	No/Yes
High nuclear-cytoplasmic ratio	No/Yes
Mitosis	No/Yes
If Yes,	
Atypical mitosis present	No/Yes

MM, malignant mesothelioma

Table 2.

Patient Demographics and Clinical Data

Variable	MMT n = 49	MME n = 6154	MMB n = 878	MMS n = 540	Comparison Test
Sex					$p < 0.0001$[a]
Male	38 (78%)	4495 (73%)	687 (78%)	445 (82%)	
Female	11 (22%)	1659 (27%)	191 (22%)	95 (18%)	
Age at diagnosis					$p = 0.002$[b]
Median	72 y	71 y	71 y	73 y	
Range	[53-88]	[13-99]	[26-94]	[40-96]	
Asbestos exposure	N = 32	N = 4131	N = 548	N = 365	$p = 0.01$[a]
No	6 (19%)	892 (22%)	88 (16%)	66 (18%)	
Yes	26 (81%)	3239 (78%)	460 (84%)	299 (82%)	
Thoracic pain	N = 32	N = 3186	N = 377	N = 279	$p < 0.0001$[a]
No	5 (17%)	822 (27%)	83 (22%)	33 (12%)	
Yes	27 (83%)	2364 (73%)	294 (78%)	246 (88%)	
Loss of performance status	N = 32	N = 3186	N = 377	N = 279	$p < 0.0001$[a]
No	6 (20%)	1338 (42%)	98 (26%)	73 (26%)	
Yes	26 (80%)	1848 (58%)	279 (74%)	206 (74%)	
Dyspnea	N = 32	N = 3186	N = 377	N = 279	$p < 0.0001$[a]
No	7 (27%)	382 (12%)	57 (16%)	59 (21%)	
Yes	25 (73%)	2804 (88%)	320 (85%)	220 (79%)	
Pleural effusion	N = 32	N = 3186	N = 377	N = 279	$p < 0.0001$[a]
No	1 (2%)	112 (4%)	13 (3%)	25 (9%)	
Yes	31 (98%)	3074 (96%)	364 (97%)	254 (91%)	

Variable	MMT n = 49	MME n = 6154	MMB n = 878	MMS n = 540	Comparison Test
Pleural thickening	N = 32	N = 3186	N = 377	N = 279	$p = 0.10^a$
No	2 (5%)	127 (4%)	11 (3%)	3 (1%)	
Yes	30 (95%)	3059 (96%)	366 (97%)	276 (99%)	
Localized mass	N = 32	N = 3186	N = 377	N = 279	$p < 0.0001^a$
No	20 (62%)	2435 (76%)	245 (65%)	157 (56%)	
Yes	12 (38%)	751 (24%)	132 (35%)	122 (44%)	
Fibrohyaline plaques	N = 32	N = 3186	N = 377	N = 279	$p < 0.0001^a$
No	17 (53%)	2038 (64%)	214 (57%)	141 (50%)	
Yes	15 (47%)	1148 (36%)	163 (43%)	138 (50%)	

Bold *p* values are significant at 5% risk level.

[a] p: χ^2 or Fisher exact bilateral test.

[b] p: Mann-Whitney test.

MMT, transitional malignant mesothelioma; MME, epithelioid malignant mesothelioma; MMB, biphasic malignant mesothelioma; MMS, sarcomatoid malignant mesothelioma.

Table 3.

Diagnosis of Histologic Types and Presence of TM in the Comparative Series of TM and Non-TM Group

Variable	Nontransitional (n = 384)	Transitional (n = 400)	Comparison test
Histologic type			-
Epithelioid	204 (53%)	-	
Biphasic	53 (14%)		
Sarcomatoid	127 (33%)		
Presence of transitional component			$p < 0.0001$[a]
No	194 (51%)	0	
Yes	190 (49%)	400 (100%)	
Presence of diffuse transitional pattern			$p < 0.0001$[a]
No	360 (94%)	91 (23%)	
Yes	24 (6%)	309 (77%)	
Presence of focal transitional pattern			$p < 0.0001$[a]
No	194 (51%)	120 (30%)	
Yes	190 (49%)	280 (70%)	

Bold *p* values are significant at 5% risk level.

[a] p: χ^2 test

TM, transitional mesothelioma.

Table 4.

Diagnosis on Criteria of Aggressiveness in the Comparative Series of TM and Non-TM Group

Variable	Non- transitional (n = 384)	Transitional (n = 400)	Comparison test
Lack of frank sarcomatous features	n = 257	n = 357	$p < 0.0001^a$
No	103 (40%)	79 (22%)	
Yes	154 (60%)	278 (78%)	
Large ovoid/nuclei/prominent nuclei	n = 267	n = 369	$p = 0.0002^a$
No	65 (24%)	47 (13%)	
Yes	202 (76%)	322 (87%)	
High nuclear-cytoplasmic ratio	n = 266	n = 368	$p = 0.30^a$
No	124 (47%)	188 (51%)	
Yes	142 (53%)	180 (49%)	
Mitosis	n = 228	n = 344	$p = 0.004^a$
No	47 (21%)	110 (32%)	
Yes	181 (79%)	234 (68%)	
When presence of mitosis, atypical mitosis	n = 163	n = 216	$p = 0.98^a$
No	54 (33%)	73 (34%)	
Yes	109 (67%)	143 (66%)	

Bold *p* values are significant at 5% risk level.

^{a}p: χ^2 test

TM, transitional mesothelioma.

Table 5.

Diagnosis Based on Cellular Structure of the TM Cells in the Comparative Series of TM and Non-TM Group

Variable	Nontransitional (n = 384)	Transitional (n = 400)	Comparison Test
Sheet cell growth	n = 296	n = 397	$p = 0.01^a$
No	50 (17%)	41 (10%)	
Yes	246 (83%)	356 (90%)	
Cohesive cells	n = 296	n = 398	$p = 0.05^a$
No	69 (23%)	68 (17%)	
Yes	227 (77%)	330 (83%)	
Well-defined borders	n = 296	n = 400	$p < 0.0001^a$
No	133 (45%)	49 (12%)	
Yes	163 (55%)	351 (88%)	
Epithelial like shape with moderate to abundant cytoplasm	n = 292	n = 400	$p < 0.0001^a$
No	82 (28%)	44 (11%)	
Yes	210 (62%)	356 (89%)	
Plump cells	n = 296	n = 400	$p < 0.0001^a$
No	62 (20%)	26 (6%)	
Yes	234 (80%)	374 (94%)	
Elongated or tapering cells	n = 218	n = 400	$p < 0.0001^a$
No	103 (24%)	20 (5%)	
Yes	165 (76%)	380 (95%)	

Bold *p* values are significant at 5% risk level.

[a] *p*: χ^2 test

TM, transitional mesothelioma.

J Thorac Oncol. Author manuscript; available in PMC 2022 February 23.

Table 6.

Results of *BAP1* and p16 Expression and *CDKN2A* (p16) Homozygous Deletion by Transitional and Nontransitional Patterns

	MMT	MME	MMB	MMS	
Variable	**n = 49**	**n = 6154**	**n = 878**	**n = 540**	**Comparison Test**
BAP1 protein	n = 34	n = 856	n = 95	n = 62	$p < 0.0001^a$
Lost	15 (44%)	558 (65%)	48 (50%)	13 (21%)	
Retained	19 (56%)	298 (35%)	47 (50%)	49 (79%)	
p16 protein	n = 34	n = 1010	n = 129	n = 104	$p < 0.0001^a$
Lost	29 (92%)	563 (56%)	94 (73%)	78 (75%)	
Retained	5 (8%)	447 (44%)	35 (27%)	26 (25%)	
p16 deletion	n = 22	n = 256	n = 97	n = 92	$p = 0.0003^a$
Homozygous deletion	16 (73%)	118 (46%)	65 (67%)	58 (63%)	
No deletion	6 (27%)	138 (54%)	32 (33%)	34 (88%)	

Bold *p* values are significant at 5% risk level.

[a] *p*: χ^2 test.

MMT, transitional malignant mesothelioma; MME, epithelioid malignant mesothelioma; MMB, biphasic malignant mesothelioma; MMS, sarcomatoid malignant mesothelioma.